Valeriani M, Barba C, Le Pera D, Restuccia D, Colicchio G, Tonali P, et al. Different neuronal contribution to N20 somatosensory evoked potential and to CO2 laser evoked potentials: an intracerebral recording study. Clin Neurophysiol 2004;115:211–6.

Valeriani M, Rambaud L, Mauguiere F. Scalp topography and dipolar source modeling of potentials evoked by CO2 laser stimulation of the hand. Electroencephalogr Clin Neurophysiol 1996;100:343–53.

Valeriani M, Restuccia D, Barba C, Le Pera D, Tonali P, Mauguiere F. Sources of cortical responses to painful CO(2) laser skin stimulation of the hand and foot in the human brain. Clin Neurophysiol 2000;111:1103–12.

Vogel H, Port JD, Lenz FA, Solaiyappan M, Krauss G, Treede RD. Dipole source analysis of laser-evoked subdural potentials recorded from parasylvian cortex in humans. J Neurophysiol 2003;89:3051–60.

Vogt BA. Pain and emotion interactions in subregions of the cingulate gyrus. Nat Rev Neurosci 2005;6:533–44.

Vogt BA, Rosene DL, Pandya DN. Thalamic and cortical afferents differentiate anterior from posterior cingulate cortex in the monkey. Science 1979;204:205–7.

Wall PD. Cord cells responding to touch, damage, and temperature of skin. J Neurophysiol 1960;23:197–210.

Watanabe S, Kakigi R, Koyama S, Hoshiyama M, Kaneoke Y. Pain processing traced by magnetoencephalography in the human brain. Brain Topogr 1998;10:255–64.

Willis WD, Trevino DL, Coulter JD, Maunz RA. Responses of primate spinothalamic tract neurons to natural stimulation of hindlimb. J Neurophysiol 1974;37:358–72.

Willis WD, Westlund KN. Neuroanatomy of the pain system and of the pathways that modulate pain. J Clin Neurophysiol 1997;14:2–31.

Yamasaki H, Kakigi R, Watanabe S, Naka D. Effects of distraction on pain perception: magneto- and electro-encephalographic studies. Brain Res Cogn Brain Res 1999;8:73–6.

Pain 123 (2006) 322–331

PAIN

www.elsevier.com/locate/pain

Multiple pathways for noxious information in the human spinal cord

Takeshi Tsuji [a,b,*], Koji Inui [a], Seiji Kojima [b], Ryusuke Kakigi [a,c]

[a] *Department of Integrative Physiology, National Institute for Physiological Sciences, Myodaiji, Okazaki 444-8585, Japan*
[b] *Department of Pediatrics, Nagoya University Graduate School of Medicine, Nagoya 466-8550, Japan*
[c] *RISTEX, Japan Science and Technology Agency, Japan*

Received 10 September 2005; received in revised form 8 March 2006; accepted 13 March 2006

Abstract

To investigate the pathways of noxious information in the spinal cord in humans, we recorded cortical potentials following the stimulation of A-delta fibers using a YAG laser applied to two cutaneous points on the back at the C7 and Th10 level, 4 cm to the right of the vertebral spinous process. A multiple source analysis showed that four sources were activated; the primary somatosensory cortex (SI), bilateral parasylvian region (Parasylvian), and cingulate cortex. The activity of the cingulate cortex had two components (N2/P2). The mean peak latencies of the activities obtained by C7 and Th10 stimulation were 166.9 and 186.0 ms (SI), 144.3 and 176.8 ms (contralateral Parasylvian), 152.7 and 185.5 ms (ipsilateral Parasylvian), 186.2 and 215.8 ms (N2), and 303.0 and 332.3 ms (P2). Estimated spinal conduction velocities (CVs) of the respective activities were 16.8, 9.3, 8.7, 10.1 and 10.7 m/s. CV of SI was significantly faster than the others ($P < 0.05$). Therefore, our results suggested that noxious signals were conveyed through at least two distinct pathways of the spinal cord probably reaching distinct groups of thalamic nuclei. Further studies are required to clarify the functional significance of these two pathways.

Keywords: Pain; Spinothalamic tracts; Conduction velocity; Electroencephalography; Laser evoked potential

1. Introduction

Noxious stimuli applied to the skin surface are detected by nociceptors in the epidermis (Burgess and Perl, 1967; Beitel and Dubner, 1976). The signals are conveyed through thinly myelinated A-delta-fibers and unmyelinated C-fibers to reach the dorsal horn of the spinal cord (Light and Perl, 1979; Sugiura et al., 1986). In the spinal cord, two different groups of neurons receive inputs from the periphery, that is, neurons in the superficial lamina (mainly lamina I) and deep lamina (mainly lamina V). Therefore, the processing of noxious signals in separate systems starts at the spinal level (Craig, 2003; Price et al., 2003). Nociceptive-specific (NS) neurons in lamina I respond to cold and noxious stimuli (Christensen and Perl, 1970; Kumazawa et al., 1975; Dostrovsky and Craig, 1996), while wide dynamic range (WDR) neurons in lamina V respond to both noxious and innocuous stimuli (Wall, 1960; Mendell, 1966; Willis et al., 1974). Then they project to distinct thalamic regions, although their terminations partly overlap (Apkarian and Hodge, 1989a). Spinothalamic neurons in lamina I mainly project to the medial thalamic nuclei and possibly to posterior part of the ventral medial nucleus (VMpo), while those in lamina V mainly project to the ventral posterior lateral nucleus (VPL) (Kenshalo et al., 1980; Ralston and Ralston, 1992; Craig et al., 1994). Furthermore, these thalamic nuclei have distinct projection sites. That is, VPL, VMpo, and medial thalamic nuclei mainly project to the primary somatosensory cortex (SI), the insula, and the anterior cingulate cortex (ACC), respectively (for review, see Treede

* Corresponding author. Tel.: +81 564 55 7814; fax: +81 564 52 7913.
E-mail address: ttsuji@nips.ac.jp (T. Tsuji).

0304-3959/$32.00
doi:10.1016/j.pain.2006.03.009

et al., 1999). Considering the different response properties of neurons and different anatomical pathways, these two streams of nociceptive processing appear to differ in function. In spite of these findings in animal studies, the functional and anatomical segregation in humans is still a subject of controversy, since less is known about segregated nociceptive processing largely due to the limitations of experimental methods. Notably, whether there are distinct pathways in the spinal cord itself is not well understood.

Therefore in the present study, we sought to clarify multiple spinal pathways for nociceptive processing in humans. We recorded cerebral evoked potentials (EPs) following Tm:YAG laser stimulation applied to two different levels of the right side of the back to measure the conduction velocity (CV) of signals in the spinothalamic tracts (STT). Previous studies in animals showed that pathways from the dorsal horn neurons in lamina I and lamina V to the thalamus had different CVs (Ferrington et al., 1987). Therefore, we considered that different pathways would have distinct CVs also in humans.

2. Methods

The experiment was performed on 10 healthy right-handed male volunteers, aged 22–36 years (mean, 29.3 ± 4.0). The study was approved in advance by the Ethics Committee of the National Institute for Physiological Sciences and written consent was obtained from all the subjects.

2.1. Noxious stimulation

For noxious stimulation, we used a Tm:YAG laser (Neurolaser, Baasel Lasertech, Germany). The wavelength was 2000 nm, pulse duration was 1 ms, and spot diameter was 6 mm. Laser stimuli were applied to two sites: the right side of the back 4 cm lateral to the 7th cervical vertebral spinous process (C7) and 10th thoracic vertebral spinous process (Th10). We chose these sites for stimulation to minimize the peripheral conduction distance of primary neurons, and stimulate the peripheral nerve of one side. In our previous report (Inui et al., 2006), we confirmed that the back is one of the cutaneous areas at which noxious stimulation evokes clear brain responses. Also, Cruccu et al. (2000) and Iannetti et al. (2003) obtained good results after noxious stimulation of the back. Histologically, the intraepidermal nerve fiber density of the trunk is higher than that of the distal leg (Lauria et al., 1999). The threshold for a pinprick sensation in the trunk is lower than that in the extremities (Agostino et al., 2000). The stimuli were delivered randomly at an interval of 10–15 s. The irradiated points were moved slightly within a transverse 4 cm area centered on the points after each stimulus to avoid tissue damage and habituation of the receptors. Subjects were asked to rate the intensity of the perceived pricking pain on a visual analogue scale (VAS, 0–10) prior to the experiment, and the stimulus intensity was adjusted to the level eliciting a VAS score of around seven.

2.2. EP recordings

Subjects lay prone on a bed and were asked to relax their muscles and keep their eyes open. The room temperature was 25 °C and sound and light were regulated. Skin temperature was kept above 30 °C (Kakigi and Shibasaki, 1991). A simultaneously recorded electro-oculogram (EOG) was used for artifact rejection. Signals were recorded with a band-pass filter of 0.1–100 Hz. The window of analysis was 600 ms including 100 ms of a prestimulus period, and the sampling rate was 1000 Hz. Laser stimuli were applied to C7 and Th10 randomly. For each site of stimulation, over 25 artifact-free trials were selected and averaged off-line. To minimize endogenous factors, subjects were asked not to predict which site would be stimulated and not to pay attention to the stimulated sites.

2.3. Source modeling

We recorded EPs using the standard 19 electrodes of the 10–20 system (Fp1, Fp2, F3, F4, F7, F8, Fz, C3, C4, Cz, T3, T4, T5, T6, P3, P4, Pz, O1, O2) and an additional 13 electrodes including FC1, FC2, C1, C2, C5, C6, T9, T10, CP1, CP2, P1, P2 and CPz (Fig. 1). The electrode impedance was always kept below 5 kΩ. We used the balanced non-cephalic reference (BNP, Stephenson and Gibbs, 1951), to reduce problems due to activities of the reference. We linked two electrodes, one from over the right sternoclavicular junction and the other from over the tip of the 7th cervical spine, and incorporated a variable resistor. By adjusting the resistance, the pickup of cardiac potentials was minimized.

Since several cortical activities following noxious stimulation overlapped temporally, we analyzed theoretical multiple source generators of EPs using the brain electric source analysis (BESA) software package (NeuroScan, Inc, Mclean, VA, USA). Model adequacy was assessed by examining: (i) percent variance; (ii) F-ratio (ratio of reduced χ^2 values before and after adding a new source); and (iii) residual waveforms

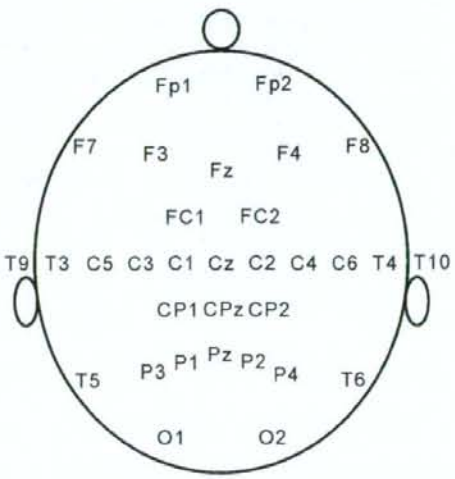

Fig. 1. Locations of the 32 electrodes.

(i.e., the difference between the recorded data and the model) as described elsewhere (Inui et al., 2004). Percent variance measures the goodness of fit (GOF) of the model comparing the recorded data and the model. The integral probability of obtaining a *F*-ratio value equal to or greater than the obtained value is calculated to evaluate whether a model with a larger number of dipoles represents a statistical improvement of the fit over a model with a smaller number of dipoles. When a *P* value was <0.05, we considered the new dipole as significant. BESA uses a spherical 4 shell model with an 85 mm radius. The spatial position of each dipole is defined by reference points on the head known as fiducials. The reference points are nasion, the left preauricular point (T9), and the right preauricular point (T10). The *x* axis is defined by the line joining T9 and T10, positive towards T10. The *y* axis is defined by the line through nasion that is perpendicular to the *x* axis (positive towards nasion). The *z* axis is perpendicular to the *x* and *y* axes, and goes up out of the head in the vicinity of Cz.

2.4. Measuring conduction velocities

The CV of a given nerve fiber can be calculated by measuring the difference in response latency of cerebral potentials between two different stimulation sites. For example, by dividing the distance between hand and arm stimulation sites by the latency difference of evoked potentials following hand and arm stimulations, one can estimate the CV of the peripheral nerve. By use of laser-evoked potentials (LEPs), the CV of A-delta fibers can be measured (Kenton et al., 1980; Bromm and Treede, 1987). By use of similar methods, CVs in STT were also measured (Kakigi and Shibasaki, 1991; Cruccu et al., 2000; Rossi et al., 2000; Qiu et al., 2001; Iannetti et al., 2003).

In the present study, the spinal conduction time was taken from the difference in the peak latency of each cortical activity between C7 and Th10 stimulation. Although the onset latency is desirable when examining the timing of the arrival of nociceptive signals in a cortical area, its determination was difficult. Therefore, we used the peak latency as in previous reports (Kakigi and Shibasaki, 1991; Cruccu et al., 2000; Rossi et al., 2000; Qiu et al., 2001; Iannetti et al., 2003). The peak latency was the latency point with the maximal amplitude. The CV was calculated by dividing the distance between C7 and Th10 by the difference in latency of each activity.

In the present study, we had an interest in the spinal conduction time, not in other conduction times. So, even though the peak latency does not directly reflect the conduction time calculated with the CV, it did not matter. For example, although the latency of P2 is too late for the CV, it would not result from the spinal cause (Kakigi and Shibasaki, 1991; Rossi et al., 2000; Iannetti et al., 2003). The latency difference could reflect the spinal conduction time.

2.5. Analysis

Data were expressed as means ± SD. The statistical significance of the peak latencies of each stimulated site and CVs was assessed with a one-way analysis of variance (ANOVA). When the *P* value was less than 0.05, a post hoc analysis with the Bonferroni and Dunn method was performed.

3. Results

Fig. 2 shows results for a representative subject. Laser stimuli applied to C7 produced an activity at around 127 ms in the parasylvian region of both hemispheres. The topography also indicated a negativity around the parietal region contralateral to the stimulated side at around 149 ms. At later latencies, a large negativity at around 175 ms followed by a larger positivity at around 320 ms was evident and corresponded to well-known N2/P2 components (Kakigi et al., 2000). These topographic findings indicated that at least four distinct sources were active during the period of analysis. Therefore, we analyzed the data using BESA to differentiate each source activity.

Isocontour maps at 127 ms in Fig. 2B show that bilateral sources around the sylvian region were active. To explain the data at this latency point, two sources were estimated to be located in the bilateral parasylvian region (Fig. 2E, a). Fig. 2C, a shows the theoretical distribution of these sources. This two-dipole model could explain 74.2% of the recorded EPs at 127 ms. Then we subtracted the theoretical waveforms of these sources from the recorded EPs (Fig. 2A, b). To explain the subtracted waveform, the best source was estimated in the midcingulate cortex (MCC) based on the recent cytoarchitectonic subdivision by Vogt (2005) (Fig. 2E, b), which appears to correspond to a region described as the anterior cingulate cortex in many previous reports. At a latency range from 175 to 450 ms, the addition of the MCC source markedly improved the fit (for example, the GOF value at 320 ms increased from 0.8% to 91.5%). We considered that this activity was compatible with the well-known N2/P2. This three-dipole model could explain 87.2% of the recorded EPs, but weak dipolar fields around the parietal region remained to be explained (Fig. 2A, c and D, a). To explain the residual waveform, the best source was estimated to be located in a parietal region slightly posterior to the central sulcus around the midline (Fig. 2E, c), which probably corresponds to the medial part of the postcentral gyrus of the contralateral hemisphere. With the addition of this source (SI source), the residual waveforms in Fig. 2A, c were almost abolished. This four-source model provided a GOF value of 90.7%.

Similar results were obtained in the remaining subjects. The mean coordinates of each dipole are shown in Table 1. The SI source was located around the midline, which was compatible with the trunk area of SI. These results were similar to the four-dipole model after stimulation of the hand reported by Tarkka and Treede (1993) and Schlereth et al. (2003). The MCC source as the major contributor to EPs following stimulation of the back was also consistent with the results reported by Iannetti et al. (2003). Accordingly, five distinct activities, SI, bilateral parasylvian activities (Pc and Pi) and MCC (N2/P2), were used to measure CVs.

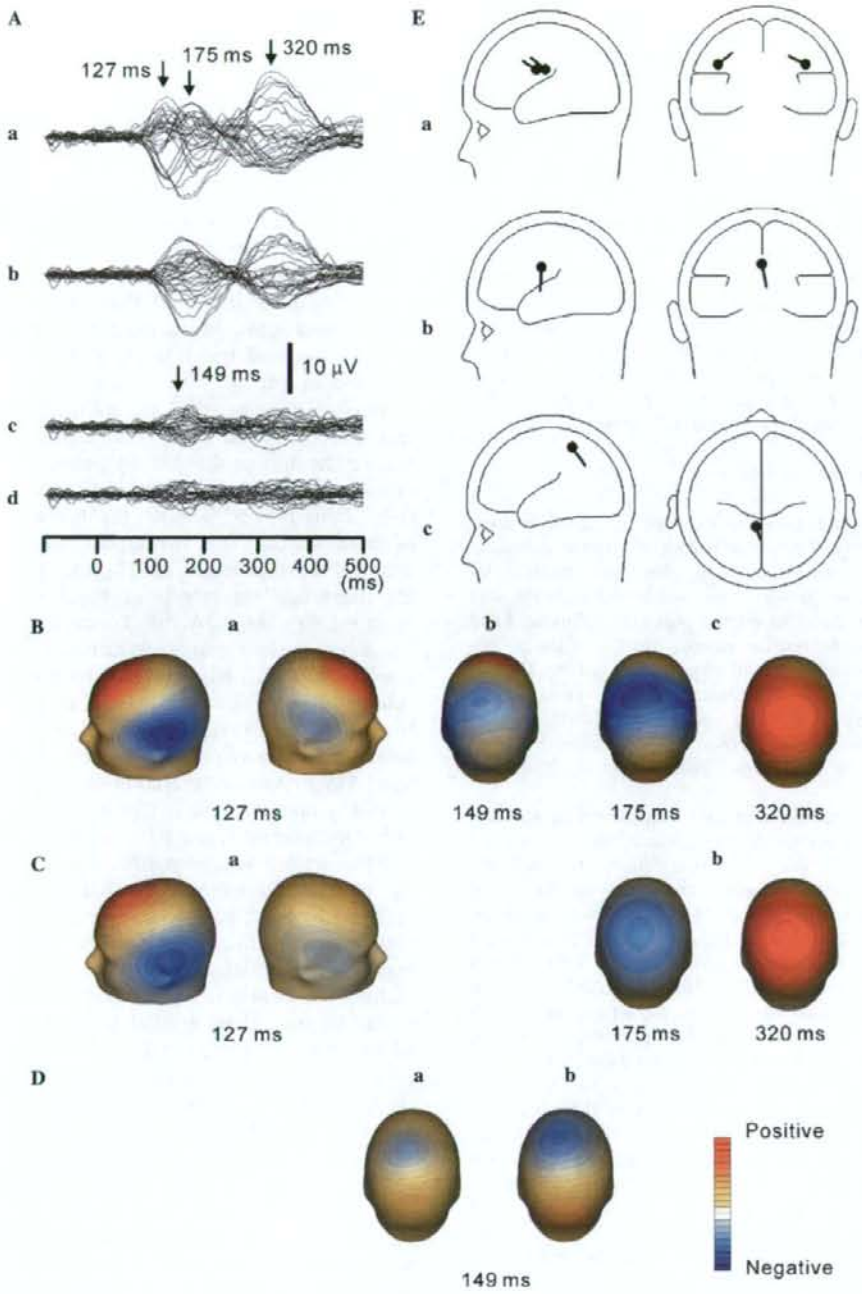

Fig. 2. Procedures of the multiple source analysis in a representative subject. First, two dipoles around the sylvian region (E, a) were estimated to explain the waveform recorded around 127 ms. B, a and C, a show isocontour maps of the recorded data and the two-dipole model at 127 ms, respectively. A, b shows the residual waveform obtained by the subtraction of the theoretical waveform due to these two sources from the recorded waveform (A, a). To explain the residual waveform (A, b), the best third source was estimated to be located in the cingulate cortex (E, b). B, c and C, b show isocontour maps of the recorded data and the third source model, respectively. A, c shows the residual waveform that remains to be explained by the three-dipole model. To explain the distribution of the residual waveform (D, a), the fourth source was estimated to lie around the medial part of the postcentral gyrus (E, c). D, b shows the theoretical field distribution of this source. After the fitting of these four sources, the residual waveform (A, d) showed no clear components.

Table 1
Locations of dipoles

	C7			Th10		
	x	*y*	*z*	*x*	*y*	*z*
SI	−4.8 ± 6.8	−16.6 ± 20.7	86.0 ± 8.4	−3.9 ± 6.5	−15.1 ± 19.1	87.4 ± 7.4
Pc	−45.3 ± 10.6	15.4 ± 4.8	56.3 ± 4.6	−45.1 ± 10.5	15.6 ± 7.2	55.6 ± 4.9
Pi	47.1 ± 12.2	15.0 ± 7.3	56.3 ± 5.7	47.6 ± 12.1	15.3 ± 7.2	56.0 ± 4.9
MCC	−3.1 ± 7.4	10.1 ± 12.9	56.8 ± 18.3	−0.6 ± 5.6	12.3 ± 15.8	59.5 ± 13.9

SI, primary somatosensory cortex; Pc, parasylvian source in the hemisphere contralateral to the stimulated side; Pi, parasylvian source in the hemisphere ipsilateral to the stimulated side; MCC, midcingulate cortex.

The peak latencies of each activity are shown in Table 2. An ANOVA showed that there was a significant difference in peak latency among the five activities following C7 stimulation ($F(1,4) = 218.8$, $P < 0.01$). The peak latency of P2 was significantly later than that of any other activities (post hoc test: $P < 0.01$), and the peak latency of N2 was also significantly later than that of SI, Pc or Pi (post hoc test: $P < 0.05$). On average, the peak latency of P2 was later than that of N2 by 116.8 ms, and in turn, the peak latency of N2 was later than that of SI, Pc and Pi by 19.3, 41.9 and 33.5 ms, respectively. The temporal relationship of each activity following Th10 stimulation was similar to that following C7 stimulation.

The estimated CVs of each activity are shown in Table 2. An ANOVA showed that there was a significant difference in CVs among the five activities ($F(1,4) = 6.4$, $P < 0.01$). The CV of SI was significantly greater than that of any other activities (post hoc test: $P < 0.05$). There was no significant difference among CVs for Pc, Pi, N2 and P2 (see Fig. 3).

4. Discussion

The present results clearly showed that at least two distinct pathways in the spinal cord transmitted noxious signals. This is the first report to confirm in the human spinal cord that nociceptive signals are processed by both the faster spinal CV pathway projecting to SI and the slower spinal CV pathway projecting to the parasylvian region and MCC.

4.1. Cortical activities

We identified activities in four cortical areas, SI, bilateral parasylvian regions and MCC, which is consistent with previous LEP studies (Tarkka and Treede, 1993; Schlereth et al., 2003). Previous LEP studies (Table 3) consistently found activities in the sylvian region. However, the locations of the parasylvian source were variable. Dipoles in electroencephalographic (EEG) and magnetoencephalographic (MEG) studies tend to be estimated in the upper bank of the sylvian fissure, while dipoles identified using subcortical and intracerebral recordings tended to be in deeper areas. MCC is an essential source in EEG studies, but not in MEG studies.

In previous studies, a somatotopic arrangement of SI activities after noxious stimulation to the hand and foot compatible with the well-known somatosensory homunculus has been reported in monkeys (Kenshalo et al., 2000) and humans (Penfield and Boldrey, 1937; Tarkka

Table 2
The peak latency of each source activity and estimated conduction velocity in the spinothalamic tract

Subject	Peak latency (ms)										Distance (cm)	Conduction velocity (m/s)				
	SI		Pc		Pi		N2		P2							
	C7	Th10	C7	Th10	C7	Th10	C7	Th10	C7	Th10		SI	Pc	Pi	N2	P2
1	157	178	146	181	153	192	187	221	285	321	28.5	13.6	8.1	7.3	8.4	7.9
2	184	207	128	149	157	184	175	194	324	350	27.5	12.0	13.1	10.2	14.5	10.6
3	180	198	144	169	152	180	171	204	327	345	26.5	14.7	10.6	9.5	8.0	14.7
4	148	173	134	170	153	183	194	216	331	354	27.2	10.9	7.6	9.1	12.4	11.8
5	161	171	150	170	155	183	194	219	283	302	26.8	26.8	13.4	9.6	10.7	14.1
6	178	190	159	184	159	187	185	214	315	336	26.0	21.7	10.4	9.3	9.0	12.4
7	171	202	139	199	149	180	188	239	293	338	27.5	8.9	4.6	8.9	5.4	6.1
8	174	187	149	186	146	199	186	205	287	322	28.5	21.9	7.7	5.4	15.0	8.1
9	144	172	140	179	136	174	165	191	278	330	27.5	9.8	7.1	7.2	10.6	5.3
10	172	182	154	181	167	193	217	255	307	325	27.8	27.8	10.3	10.7	7.3	15.4
Mean	166.9	186.0	144.3	176.8	152.7	185.5	186.2	215.8	303.0	332.3	27.4	16.8	9.3	8.7	10.1	10.7
SD	13.7	13.0	9.3	13.3	8.2	7.4	14.5	19.6	20.2	15.6	0.8	7.1	2.8	1.6	3.1	3.6

SI, primary somatosensory cortex; Pc, parasylvian source in the hemisphere contralateral to the stimulated side; Pi, parasylvian source in the hemisphere ipsilateral to the stimulated side.

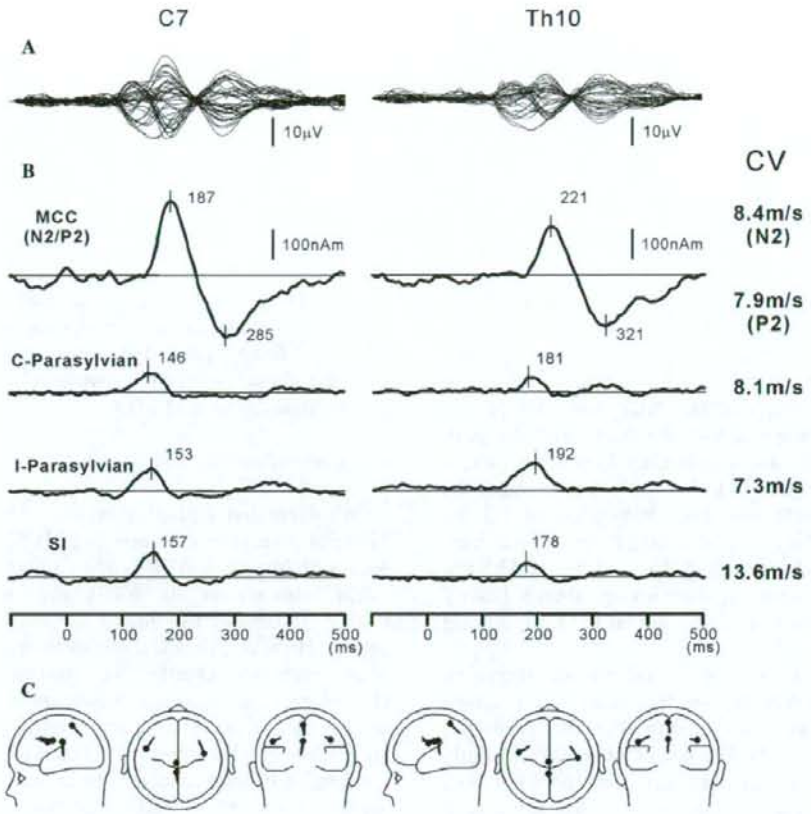

Fig. 3. Estimation of conduction velocity of each source activity in the spinal cord in a single subject. (A) Superimposed waveforms of evoked potentials following C7 (left) and Th10 (right) stimulation. (B) Time course of each cortical activity obtained by a multiple source analysis. (C) Schematic drawings of the location and orientation of each source. Estimated conduction velocity (CV) of each activity is shown. Note the similar latency difference between C7 and Th10 stimulation with the exception that the difference is smaller for the SI activity than the other source activities.

and Treede, 1993; Bingel et al., 2004; Ogino et al., 2005). These studies showed that the hand was represented in the lateral part of the postcentral gyrus and the foot, near the midline. These results imply that the pain system employs a body surface map in SI that is similar to the somatosensory homunculus. Since the representation of the trunk in SI in the somatosensory system is located around the midline, our results seem to support this idea. However, the precise location of nociceptive neurons in SI was slightly posterior to area 3b and probably in area 1, area 2 or the posterior parietal cortex in animals (Kenshalo and Isensee, 1983) and human studies (Kanda et al., 2000; Ploner et al., 2000; Inui et al., 2003; Ohara et al., 2004; Valeriani et al., 2004). The timing of SI activation in the present study was consistent with previous EEG and MEG studies (Tarkka and Treede, 1993; Ploner et al., 1999; Inui et al., 2003).

Our multiple source analysis showed that bilateral parasylvian EP components come from the sylvian region. Although previous LEP studies agreed that this activity was generated in the secondary somatosensory cortex (SII) area (Tarkka and Treede, 1993; Bromm and Chen, 1995; Kakigi et al., 1995; Valeriani et al., 1996), recent subdural LEP studies showed that it was generated in the frontoparietal operculum overlying insula, not in the parietal operculum overlying SII (Lenz et al., 2000; Vogel et al., 2003). In functional magnetic resonance imaging (fMRI) studies, both SII and the insula were activated by noxious stimuli (Brooks et al., 2002; Bingel et al., 2003). Our previous MEG study using noxious intraepidermal electrical stimulation (Inui et al., 2003) showed that the insula was activated almost simultaneously with SII, although the results could not be directly compared with those of the present study because of different stimulus and recording conditions. The precise anatomical area responsible for this activity has not yet been determined. Therefore, we considered that parasylvian activity in the present study might be a summation of several temporally overlapping activities from the sylvian region.

Table 3
Source locations in previous studies (scalp EEG, MEG, subdural, and intracerebral)

Reference	Recording	Laser	Activated cortical area
Tarkka and Treede (1993)	EEG	CO_2	SI, SII, ACC
Bromm and Chen (1995)	EEG	CO_2	SII, ACC, frontal cortex
Kakigi et al. (1995)	MEG	CO_2	SII
Valeriani et al. (1996)	EEG	CO_2	SII, CC, mesial-temporal cortex
Watanabe et al. (1998)	MEG	CO_2	SII, amygdala-hippocampal formation
Lenz et al. (1998a)	Subdural	CO_2	Parietal operculum and/or insula
Lenz et al. (1998b)	Subdural	CO_2	ACC
Yamasaki et al. (1999)	MEG	CO_2	SII
Ploner et al. (1999)	MEG	YAG	SI, SII
Frot et al. (1999)	Intracerebral	CO_2	Frontoparietal operculum
Valeriani et al. (2000)	EEG	CO_2	SII, CC, insular-temporal cortex
Ploner et al. (2000)	MEG	YAG	SI (area 1), SII
Kanda et al. (2000)	MEG	CO_2	SI (area 1), SII
Lenz et al. (2000)	Subdural	CO_2	Parietal operculum–insula
Timmermann et al. (2001)	MEG	YAG	SI, SII
Frot et al. (2001)	Intracerebral	CO_2	Frontoparietal operculum
Ploner et al. (2002)	MEG	YAG	SI, SII, ACC
Iannetti et al. (2003)	EEG	CO_2	ACC
Schlereth et al. (2003)	EEG	YAG	SI, ACC, operculum
Vogel et al. (2003)	Subdural	CO_2	Frontoparietal operculum
Frot and Mauguiere (2003)	Intracerebral	CO_2	Operculum–insula
Valeriani et al. (2004)	Subdural	CO_2	SI (area 1, 2 or posterior parietal cortex)
Ohara et al. (2004)	Subdural	YAG	SI (not area 3b or 1), parasylvian area, ACC, SMA

SI, primary somatosensory cortex; SII, secondary somatosensory cortex; ACC, anterior cingulate cortex; SMA, supplementary motor area.

The main source generator was located in MCC, also in accordance with previous reports (Iannetti et al., 2003). Activation in these areas following noxious stimuli is consistent with fMRI studies (Bornhovd et al., 2002). Therefore, these five activities (SI, Pc, Pi, N2 and P2) were consistent with previous studies. We measured CVs of the STT using these five activities.

4.2. Methodological considerations when measuring CV

CVs of noxious signals in the human spinal cord were reported for the first time by Kakigi and Shibasaki (1991). They estimated CV by comparing the latencies of P2 following laser stimulation to the hand and foot. Although their method was confirmed later by Rossi et al. (2000), its peripheral component was not negligible. Recently, Cruccu et al. (2000) measured CV using EPs after stimulation of the dorsal midline. Since the back midline has the shortest conduction distance from the stimulated point to the spinal cord, this method has the advantage of reducing the peripheral components. In the present study, we stimulated two different levels of the right side of the back 4 cm lateral to the midline. This method had an additional advantage over previous studies in that it activated nociceptors belonging to the peripheral nerve of one side. Since noxious stimuli activate several cortical areas bilaterally with a 15–20 ms delay for the ipsilateral activity (Inui et al., 2003), the evoked response should be very complicated when stimuli are applied to the midline. That is, responses in one hemisphere contain both contralateral and ipsilateral responses due to the stimulation of peripheral nerves of both sides. Another methodological advantage of this study was the random stimulation paradigm. The EP waveform is substantially affected by level of arousal, attention and expectancy (Kakigi et al., 2000). Our method could minimize such effects.

4.3. CV in the spinal cord

The estimated CVs in the spinal cord following noxious stimulation in the present study were 8.7–16.8 m/s. The CVs calculated from the peak latency of N2 (Cruccu et al., 2000), P2 (Kakigi and Shibasaki, 1991; Rossi et al., 2000) and N1/P1 (Rossi et al., 2000) were 21, 10 (8–12) and 10.0 m/s, respectively. Therefore, values in the present study were approximately consistent with those in other studies. The CV for the SI activity has not been reported previously.

4.4. Two pathways in the STT

The STT neurons are functionally separated into NS and WDR neurons. The locations are also different, namely, NS cells are mainly located in lamina I and WDR cells are mainly present in lamina V. Axons of NS and WDR cells ascend in different parts of the STT (Apkarian and Hodge, 1989b; Craig, 2003). Furthermore, NS and WDR cells have distinct projection

targets in the thalamus, although their terminations partly overlap (Apkarian and Hodge, 1989a; Willis and Westlund, 1997). As for the CV, signals of WDR cells conduct in the STT significantly faster than those of NS cells in monkeys (Ferrington et al., 1987). In this study, the CV for SI was significantly faster than that of any other activity, implying that activation in SI came from WDR cells. This notion is consistent with the fact that lamina V WDR neurons predominantly project to VPL and in turn, VPL predominantly projects to SI (Kenshalo et al., 1980), and that the majority of nociceptive neurons both in VPL (Kenshalo et al., 1980) and in SI (Kenshalo and Isensee, 1983) are of the WDR type. Based on comparisons of neurophysiological data between humans and monkeys (Mayer et al., 1975; Price and Mayer, 1975), it has been demonstrated that WDR cells are responsible for the sensory aspect of pain.

On the other hand, signals from lamina I NS neurons ascend through the STT with a slower CV to reach the insula (Friedman and Murray, 1986) or cingulate cortex (Vogt et al., 1979) via medial nuclei of the thalamus and possibly VMpo (Ralston and Ralston, 1992; Craig et al., 1994; Craig, 2004). Therefore, MCC with a slower CV in the spinal cord in this study appeared to come from lamina I NS neurons. This idea is supported by the finding in a unitary recording study in animals (Koyama et al., 1998) and humans (Hutchison et al., 1999) that the cingulate cortex contains neurons that respond to noxious stimuli exclusively.

As for the parasylvian activity, various areas around the sylvian fissure have been reported as responsible (Table 3). If parasylvian activities reflect SII activity, our finding that the parasylvian activity had a slower spinal CV than the SI activity is congruent with the findings that VPI receives input from neurons in both lamina I and lamina V (Apkarian and Shi, 1994), and that the nociceptive neurons in VPI (Apkarian and Shi, 1994) and SII (Dong et al., 1989) are of both WDR and NS types. If parasylvian activities reflect the insular activity, the present findings are consistent with the lamina I NS cells-VMpo-insula pathway proposed by Craig et al. (1994). In the thalamus, intralaminar nuclei also relay noxious information from STT neurons to the sensory cortex. For example, the centrolateral nucleus (CL) receives inputs from STT neurons and projects to SI (Gindold et al., 1991) and SII (Stevens et al., 1993). Since a large percentage of SII-projecting thalamocortical neurons do not receive direct inputs from the spinal cord (Stevens et al., 1993), polysynaptic pathways to the thalamus, such as spinoreticulothalamic projections to the intralaminar nuclei, are possible. The present results could not clarify which spinal pathway with a slow CV is responsible for the parasylvian activity.

Acknowledgement

This study was carried out as a part of "Ground-based Research Announcement for Space Utilization" promoted by Japan Space Forum.

References

Agostino R, Cruccu G, Iannetti G, Romaniello A, Truini A, Manfredi M. Topographical distribution of pinprick and warmth thresholds to CO2 laser stimulation on the human skin. Neurosci Lett 2000;285:115–8.

Apkarian AV, Hodge CJ. Primate spinothalamic pathways: III. Thalamic terminations of the dorsolateral and ventral spinothalamic pathways. J Comp Neurol 1989a;288:493–511.

Apkarian AV, Hodge CJ. Primate spinothalamic pathways: II. The cells of origin of the dorsolateral and ventral spinothalamic pathways. J Comp Neurol 1989b;288:474–92.

Apkarian AV, Shi T. Squirrel monkey lateral thalamus. I. Somatic nociresponsive neurons and their relation to spinothalamic terminals. J Neurosci 1994;14:6779–95.

Beitel RE, Dubner R. Response of unmyelinated (C) polymodal nociceptors to thermal stimuli applied to monkey's face. J Neurophysiol 1976;39:1160–75.

Bingel U, Lorenz J, Glauche V, Knab R, Glascher J, Weiller C, Buchel C. Somatotopic organization of human somatosensory cortices for pain: a single trial fMRI study. Neuroimage 2004;23:224–32.

Bingel U, Quante M, Knab R, Bromm B, Weiller C, Buchel C. Single trial fMRI reveals significant contralateral bias in responses to laser pain within thalamus and somatosensory cortices. Neuroimage 2003;18:740–8.

Bornhovd K, Quante M, Glauche V, Bromm B, Weiller C, Buchel C. Painful stimuli evoke different stimulus–response functions in the amygdala, prefrontal, insula and somatosensory cortex: a single-trial fMRI study. Brain 2002;125:1326–36.

Bromm B, Chen AC. Brain electrical source analysis of laser evoked potentials in response to painful trigeminal nerve stimulation. Electroencephalogr Clin Neurophysiol 1995;95:14–26.

Bromm B, Treede RD. Pain related cerebral potentials: late and ultralate components. Int J Neurosci 1987;33:15–23.

Brooks JC, Nurmikko TJ, Bimson WE, Singh KD, Roberts N. fMRI of thermal pain: effects of stimulus laterality and attention. Neuroimage 2002;15:293–301.

Burgess PR, Perl ER. Myelinated afferent fibers responding specifically to noxious stimulation of the skin. J Physiol 1967;190:541–62.

Christensen BN, Perl ER. Spinal neurons specifically excited by noxious or thermal stimuli: marginal zone of the dorsal horn. J Neurophysiol 1970;33:293–307.

Craig AD. Pain mechanisms: labeled lines versus convergence in central processing. Annu Rev Neurosci 2003;26:1–30.

Craig AD. Distribution of trigeminothalamic and spinothalamic lamina I terminations in the macaque monkey. J Comp Neurol 2004;477:119–48.

Craig AD, Bushnell MC, Zhang ET, Blomqvist A. A thalamic nucleus specific for pain and temperature sensation. Nature 1994;372:770–3.

Cruccu G, Iannetti GD, Agostino R, Romaniello A, Truini A, Manfredi M. Conduction velocity of the human spinothalamic tract as assessed by laser evoked potentials. Neuroreport 2000;11:3029–32.

Dong WK, Salonen LD, Kawakami Y, Shiwaku T, Kaukoranta EM, Martin RF. Nociceptive responses of trigeminal neurons in SII-7b cortex of awake monkeys. Brain Res 1989;484:314–24.

Dostrovsky JO, Craig AD. Cooling-specific spinothalamic neurons in the monkey. J Neurophysiol 1996;76:3656–65.

Ferrington DG, Sorkin LS, Willis WD. Responses of spinothalamic tract cells in the superficial dorsal horn of the primate lumbar spinal cord. J Physiol 1987;388:681–703.

Friedman DP, Murray EA. Thalamic connectivity of the second somatosensory area and neighboring somatosensory fields of the lateral sulcus of the macaque. J Comp Neurol 1986;252:348–73.

Frot M, Garcia-Larrea L, Guenot M, Mauguiere F. Responses of the supra-sylvian (SII) cortex in humans to painful and innocuous stimuli. A study using intra-cerebral recordings. Pain 2001;94:65–73.

Frot M, Mauguiere F. Dual representation of pain in the operculo–insular cortex in humans. Brain 2003;126:438–50.

Frot M, Rambaud L, Guenot M, Mauguiere F. Intracortical recordings of early pain-related CO2-laser evoked potentials in the human second somatosensory (SII) area. Clin Neurophysiol 1999;110:133–45.

Gindold SI, Ggreenspan JD, Apkarian AV. Anatomic evidence of nociceptive inputs to primary somatosensory cortex: relationship between spinothalamic terminals and thalamocortical cells in squirrel monkeys. J Comp Neurol 1991;308:467–90.

Hutchison WD, Davis KD, Lozano AM, Tasker RR, Dostrovsky JO. Pain-related neurons in the human cingulate cortex. Nat Neurosci 1999;2:403–5.

Iannetti GD, Truini A, Romaniello A, Galeotti F, Rizzo C, Manfredi M, et al. Evidence of a specific spinal pathway for the sense of warmth in humans. J Neurophysiol 2003;89:562–70.

Inui K, Tran TD, Qiu Y, Wang X, Hoshiyama M, Kakigi R. A comparative magnetoencephalographic study of cortical activations evoked by noxious and innocuous somatosensory stimulations. Neuroscience 2003;120:235–48.

Inui K, Tsuji T, Kakigi R. Temporal analysis of cortical mechanisms for pain relief by tactile stimuli in humans. Cereb Cortex 2006;16:355–65.

Inui K, Wang X, Tamura Y, Kaneoke Y, Kakigi R. Serial processing in the human somatosensory system. Cereb Cortex 2004;14:851–7.

Kakigi R, Koyama S, Hoshiyama M, Kitamura Y, Shimojo M, Watanabe S. Pain-related magnetic fields following painful CO2 laser stimulation in man. Neurosci Lett 1995;192:45–8.

Kakigi R, Shibasaki H. Estimation of conduction velocity of the spinothalamic tract in man. Electroencephalogr Clin Neurophysiol 1991;80:39–45.

Kakigi R, Watanabe S, Yamasaki H. Pain-related somatosensory evoked potentials. J Clin Neurophysiol 2000;17:295–308.

Kanda M, Nagamine T, Ikeda A, Ohara S, Kunieda T, Fujiwara N, et al. Primary somatosensory cortex is actively involved in pain processing in human. Brain Res 2000;853:282–9.

Kenshalo DR, Giesler GJ, Leonard RB, Willis WD. Responses of neurons in primate ventral posterior lateral nucleus to noxious stimuli. J Neurophysiol 1980;43:1594–614.

Kenshalo DR, Isensee O. Responses of primate SI cortical neurons to noxious stimuli. J Neurophysiol 1983;50:1479–96.

Kenshalo DR, Iwata K, Sholas M, Thomas DA. Response properties and organization of nociceptive neurons in area 1 of monkey primary somatosensory cortex. J Neurophysiol 2000;84:719–29.

Kenton B, Coger R, Crue B, Pinsky J, Friedman Y, Carmon A. Peripheral fiber correlates to noxious thermal stimulation in humans. Neurosci Lett 1980;17:301–6.

Koyama T, Tanaka YZ, Mikami A. Nociceptive neurons in the macaque anterior cingulate activate during anticipation of pain. Neuroreport 1998;9:2663–7.

Kumazawa T, Perl ER, Burgess PR, Whitehorn D. Ascending projections from marginal zone (lamina I) neurons of the spinal dorsal horn. J Comp Neurol 1975;162:1–11.

Lauria G, Holland N, Hauer P, Cornblath DR, Griffin JW, McArthur JC. Epidermal innervation: changes with aging, topographic location, and in sensory neuropathy. J Neurol Sci 1999;164:172–8.

Lenz FA, Krauss G, Treede RD, Lee JL, Boatman D, Crone N, et al. Different generators in human temporal–parasylvian cortex account for subdural laser-evoked potentials, auditory-evoked potentials, and event-related potentials. Neurosci Lett 2000;279:153–6.

Lenz FA, Rios M, Chau D, Krauss GL, Zirh TA, Lesser RP. Painful stimuli evoke potentials recorded from the parasylvian cortex in humans. J Neurophysiol 1998a;80:2077–88.

Lenz FA, Rios M, Zirh A, Chau D, Krauss G, Lesser RP. Painful stimuli evoke potentials recorded over the human anterior cingulate gyrus. J Neurophysiol 1998b;79:2231–4.

Light AR, Perl ER. Spinal termination of functionally identified primary afferent neurons with slowly conducting myelinated fibers. J Comp Neurol 1979;186:133–50.

Mayer DJ, Price DD, Becker DP. Neurophysiological characterization of the anterolateral spinal cord neurons contributing to pain perception in man. Pain 1975;1:51–8.

Mendell LM. Physiological properties of unmyelinated fiber projection to the spinal cord. Exp Neurol 1966;16:316–32.

Ogino Y, Nemoto H, Goto F. Somatotopy in human primary somatosensory cortex in pain system. Anesthesiology 2005;103:821–7.

Ohara S, Crone NE, Weiss N, Treede RD, Lenz FA. Cutaneous painful laser stimuli evoke responses recorded directly from primary somatosensory cortex in awake humans. J Neurophysiol 2004;91:2734–46.

Penfield W, Boldrey E. Somatic motor and sensory representation in the cerebral cortex of man as studied by electrical stimulation. Brain 1937;60:389–443.

Ploner M, Gross J, Timmermann L, Schnitzler A. Cortical representation of first and second pain sensation in humans. Proc Natl Acad Sci USA 2002;99:12444–8.

Ploner M, Schmitz F, Freund HJ, Schnitzler A. Parallel activation of primary and secondary somatosensory cortices in human pain processing. J Neurophysiol 1999;81:3100–4.

Ploner M, Schmitz F, Freund HJ, Schnitzler A. Differential organization of touch and pain in human primary somatosensory cortex. J Neurophysiol 2000;83:1770–6.

Price DD, Greenspan JD, Dubner R. Neurons involved in the exteroceptive function of pain. Pain 2003;106:215–9.

Price DD, Mayer DJ. Neurophysiological characterization of the anterolateral quadrant neurons subserving pain in *M. mulatta*. Pain 1975;1:59–72.

Qiu Y, Inui K, Wang X, Tran TD, Kakigi R. Conduction velocity of the spinothalamic tract in humans as assessed by CO2 laser stimulation of C-fibers. Neurosci Lett 2001;311:181–4.

Ralston HJ, Ralston DD. The primate dorsal spinothalamic tract: evidence for a specific termination in the posterior nuclei (Po/SG) of the thalamus. Pain 1992;48:107–18.

Rossi P, Serrao M, Amabile G, Parisi L, Pierelli F, Pozzessere G. A simple method for estimating conduction velocity of the spinothalamic tract in healthy humans. Clin Neurophysiol 2000;111:1907–15.

Schlereth T, Baumgartner U, Magerl W, Stoeter P, Treede RD. Left-hemisphere dominance in early nociceptive processing in the human parasylvian cortex. Neuroimage 2003;20:441–54.

Stephenson WA, Gibbs FA. A balanced non-cephalic reference electrode. Electroencephalogr Clin Neurophysiol 1951;3:237–40.

Stevens RT, London SM, Apkarian AV. Spinothalamocortical projections to the secondary somatosensory cortex (SII) in squirrel monkey. Brain Res 1993;631:241–6.

Sugiura Y, Lee CL, Perl ER. Central projections of identified, unmyelinated (C) afferent fibers innervating mammalian skin. Science 1986;234:358–61.

Tarkka IM, Treede RD. Equivalent electrical source analysis of pain-related somatosensory evoked potentials elicited by a CO2 laser. J Clin Neurophysiol 1993;10:513–9.

Timmermann L, Ploner M, Haucke K, Schmitz F, Baltissen R, Schnitzler A. Differential coding of pain intensity in the human primary and secondary somatosensory cortex. J Neurophysiol 2001;86:1499–503.

Treede RD, Kenshalo DR, Gracely RH, Jones AK. The cortical representation of pain. Pain 1999;79:105–11.

Valeriani M, Barba C, Le Pera D, Restuccia D, Colicchio G, Tonali P, et al. Different neuronal contribution to N20 somatosensory evoked potential and to CO2 laser evoked potentials: an intracerebral recording study. Clin Neurophysiol 2004;115:211–6.

Valeriani M, Rambaud L, Mauguiere F. Scalp topography and dipolar source modeling of potentials evoked by CO2 laser stimulation of the hand. Electroencephalogr Clin Neurophysiol 1996;100:343–53.

Valeriani M, Restuccia D, Barba C, Le Pera D, Tonali P, Mauguiere F. Sources of cortical responses to painful CO(2) laser skin stimulation of the hand and foot in the human brain. Clin Neurophysiol 2000;111:1103–12.

Vogel H, Port JD, Lenz FA, Solaiyappan M, Krauss G, Treede RD. Dipole source analysis of laser-evoked subdural potentials recorded from parasylvian cortex in humans. J Neurophysiol 2003;89:3051–60.

Vogt BA. Pain and emotion interactions in subregions of the cingulate gyrus. Nat Rev Neurosci 2005;6:533–44.

Vogt BA, Rosene DL, Pandya DN. Thalamic and cortical afferents differentiate anterior from posterior cingulate cortex in the monkey. Science 1979;204:205–7.

Wall PD. Cord cells responding to touch, damage, and temperature of skin. J Neurophysiol 1960;23:197–210.

Watanabe S, Kakigi R, Koyama S, Hoshiyama M, Kaneoke Y. Pain processing traced by magnetoencephalography in the human brain. Brain Topogr 1998;10:255–64.

Willis WD, Trevino DL, Coulter JD, Maunz RA. Responses of primate spinothalamic tract neurons to natural stimulation of hindlimb. J Neurophysiol 1974;37:358–72.

Willis WD, Westlund KN. Neuroanatomy of the pain system and of the pathways that modulate pain. J Clin Neurophysiol 1997;14:2–31.

Yamasaki H, Kakigi R, Watanabe S, Naka D. Effects of distraction on pain perception: magneto- and electro-encephalographic studies. Brain Res Cogn Brain Res 1999;8:73–6.

Cerebral Cortex March 2006;16:355–365
doi:10.1093/cercor/bhi114
Advance Access publication May 18, 2005

Temporal Analysis of Cortical Mechanisms for Pain Relief by Tactile Stimuli in Humans

Koji Inui, Takeshi Tsuji and Ryusuke Kakigi

Department of Integrative Physiology, National Institute for Physiological Sciences, Myodaiji, Okazaki 444-8585, Japan

The mechanisms by which vibrotactile stimuli relieve pain are not well understood, especially in humans. We recorded cortical magnetic responses to paired noxious (intra-epidermal electrical stimulation, IES) and innocuous (transcutaneous electrical stimulation, TS) stimuli applied to the back at a conditioning–test interval (CTI) of −500 to 500 ms. Results showed that IES-induced responses were remarkably attenuated when TS was applied 20–60 ms later and 0–500 ms earlier than IES (CTI = −60 to 500 ms). Since the signals evoked by IES reached the spinal cord (CTI = −60 to −20 ms conditions) and the cortex (−60 and −40 ms condition) earlier than those evoked by TS, the present results indicate that cortical responses to noxious stimuli can be inhibited by innocuous tactile stimuli at the cortical level, with minimal contribution at the spinal level.

Keywords: intra-epidermal electrical stimulation, magnetoencephalogram, pain relief, transcutaneous electrical stimulation, vibrotactile stimuli

Introduction

Pain relief by vibrotactile stimuli is a well-known phenomenon. Although vibrotactile stimuli actually reduce experimental pain in animals (Woolf *et al.*, 1977) and humans (Wall and Cronly-Dillon, 1960), and pathological pain in patients (Wall and Sweet, 1967; Meyer and Fields, 1972), the underlying mechanisms of this inhibition are still largely unknown. Notably, whether such an inhibition of nociception occurs at the cortical level has not been investigated at all. Many previous studies have considered the dorsal horn of the spinal cord as an important site for this phenomenon where large myelinated fiber inputs are said to affect the central transmission of signals from nociceptors (Melzack and Wall, 1965). In the present study, we demonstrate that cortical responses to noxious stimuli can be substantially inhibited by innocuous tactile stimuli with minimal contribution at the periphery or spinal cord.

Materials and Methods

Nine healthy male volunteers aged 24–40 (mean 31.1) years participated in this study. The study was approved in advance by the Ethical Committee of the National Institute for Physiological Sciences and written consent was obtained from all the subjects. Experiments were conducted according to the Declaration of Helsinki.

Stimulation

For a test noxious stimulation, we used an intra-epidermal electrical stimulation (IES) method that we recently developed (Inui *et al.*, 2002a) for the selective stimulation of cutaneous A-delta fibers. However, the original method was modified slightly to provide high selectivity for the activation of nociceptors at a stronger intensity of stimulation than that used in previous studies (Inui *et al.*, 2002a,b, 2003a,b). We used a stainless steel concentric bipolar needle electrode (patent pending) for IES. The anode was an outer ring 1.2 mm in diameter and the cathode was an inner needle that protruded 0.2 mm from the outer ring. By pressing the electrode against the skin gently, the needle tip was inserted in the epidermis and superficial part of the dermis where nociceptors are located, while the outer ring was attached to the skin surface. Two electrodes 5 mm apart were used for augmentation of the response. The two electrodes were placed in parallel with the midline of the back. The electrical stimulus was current constant double pulses at 100 Hz with a 0.5 ms duration, and was applied to the right side of the back 4 cm lateral to the ninth thoracic vertebral spinous process. We chose this point since (i) the area around the back's midline is suitable for minimizing the conduction distance from the point of stimulation to the spinal cord; (ii) we wanted to stimulate the peripheral nerve of one side; and (iii) a lower point than the Th9 level would mean a longer conduction distance to the spinal cord while a higher point caused magnetic noise related to thoracic movements, that is, the stimulation electrode attached to the back moved with respiration and produced magnetic noise. The current intensity was at a level producing a definite pain sensation of ~40–60 in the visual analogue scale (VAS, 0–100) in each subject, where 0 represented no painful sensation and 100 represented an imaginary intolerable pain sensation. The mean stimulus intensity was 0.3 ± 0.08 mA. IES did not cause flare reactions around the electrode, an indication of C-fiber activation, like in our previous study (Inui *et al.*, 2002a).

For a conditioning tactile stimulation, similar cutaneous sites were stimulated using a bipolar felt tip electrode (NM-420S, NihonKoden, Tokyo), 0.9 mm in diameter with a distance of 23 mm between the anode and cathode (transcutaneous electrical stimulation, TS). The felt tip electrode was placed just lateral to the concentric electrodes, and the center of them was 1 cm apart. The stimulus was double pulses at 100 Hz with 0.5 ms duration and the stimulus intensity was three times that of the sensory threshold (1.4 ± 0.2 mA) in each subject. Clear tactile sensations were elicited without any painful sensations using these stimulus parameters.

There were 13 stimulus conditions: control TS (conditioning stimulus alone), control IES (test stimulus alone) and 11 paired stimulus (IES + TS) conditions. In the eleven IES + TS conditions, paired stimuli were delivered with conditioning-test intervals (CTIs) of −500, −300, −100, −60, −40, −20, 0, 50, 100, 300 and 500 ms. Since the distance between the stimulus point and the corresponding level of the spinal cord is ~10 cm, it takes 1.7 ms for signals evoked by TS to reach the spinal cord at a conduction velocity of 60 m/s (A-beta fiber), while it takes 6.7 ms for signals due to ES at 15 m/s (A-delta fiber) (Inui *et al.*, 2002a,b). Therefore, in the IES + TS −500 to −20 ms conditions, signals caused by IES are expected to reach the spinal cord earlier than those due to TS. Signals conveyed through peripheral A-beta and A-delta fibers also ascend in the spinal cord at different conduction velocities: A-beta fiber signals at 50–60 m/s and A-delta fiber signals at 8–10 m/s (Kakigi and Shibasaki, 1991). Given that the respective velocity is 60 and 9 m/s and the length of the spinal cord between C1 and T9 is 30 cm, the conduction time through the spinal cord in this study is 5 ms for TS and 33.3 ms for IES. Given the conduction time in the periphery and spinal cord, the difference in response latency at the cortex for TS and IES is expected to be ~33 ms. This means that in the IES + TS −500 to −40 ms conditions, signals due to IES reach the cortex earlier than those due to TS.

Pain Rating

First, we compared pain ratings among the control (IES) and 11 IES + TS conditions to examine whether and how the conditioning tactile stimuli affect the intensity of the perceived pain sensation. The stimuli of twelve conditions were presented randomly at an interval of ~5 s and subjects assessed the intensity of the pain of each stimulus based on VAS (0–100). Ten trials were performed for each condition and the mean value was used for the analysis.

MEG Recording and Analysis

Because of the long experiment time, the MEG experiment was separated into two sessions. IES + TS conditions with CTIs of –40 to 500 ms were examined in the first session, and IES + TS conditions with CTIs of –500 to –60 ms in the second session. Therefore, there were nine conditions in the first session: control IES, control TS and seven IES + TS conditions with CTIs of –40, –20, 0, 50, 100, 300 and 500 ms. In the second session, there were six conditions: control IES, control TS and four IES + TS conditions with CTIs of –500, –300, –100 and –60 ms. The two sessions were performed on different days. Somatosensory evoked magnetic fields (SEFs) were recorded using a dual 37-channel axial-type first-order biomagnetometer (Magnes, Biomagnetic Technologies, San Diego, CA) as described previously (Kakigi *et al.*, 2000). The probes were centered on the C3 and C4 positions as based on the International 10/20 System. The SEFs were recorded with a filter of 0.1–200 Hz at a sampling rate of 1048 Hz, and then filtered offline with a bandpass of 0.5–150 Hz. Sweeps were triggered by the conditioning stimulus (TS) in the first session and by the test stimulus (IES) in the second session. The window of analysis was from 150 ms before to 800 ms after the conditioning stimulus, and the prestimulus period was used as the DC baseline. The stimuli of various conditions were presented randomly at an interval of 3–5 s. For each condition, 50 artifact-free trials were collected. Throughout the MEG experiment, subjects were instructed to look at a fixation point presented 1m in front of them.

Since magnetic fields recorded in the IES +TS conditions were a mixture of TS- and IES-evoked responses, we subtracted the control TS-induced response from the response recorded in the IES + TS conditions to obtain the actual IES-evoked response. Then we calculated the root mean square (RMS) across all 74 channels of the subtracted waveform to compare the amplitude of the IES-evoked response among conditions. This method is easy to perform and the results are easy to understand. This method is based on the assumption that the TS-evoked response is not influenced by concomitant IES. However, in some IES + TS conditions, the TS-evoked cortical response was substantially affected by a preceding IES as will be described below. Therefore, we then calculated how the TS- and IES-evoked responses explain the waveforms of the IES + TS conditions using a least squares fit. Since the waveform for a IES + TS condition is the sum of the waveforms of IES and TS with various ratios, it can be expressed as

$$f(\mathrm{IES+TS}) = a \times f(\mathrm{TS}) + b \times f(\mathrm{IES}), \quad 0 \le a, b \le 1$$

where a and b are coefficients for TS and IES, respectively. The values of a and b indicate to what extent TS and IES contribute to the activity in the IES + TS conditions. When a is much larger than b, TS contributes to the waveform much more than IES, and vice versa. To obtain the best explanation of f(IES + TS), coefficients a and b must minimize the sum difference square,

$$\sum_{i=1}^{74} (\mathrm{IES+TS}_i - a\mathrm{TS}_i - b\mathrm{IES}_i)^2$$

where $\mathrm{IES+TS}_i$ are values for an IES + TS condition, TS_i are values for TS, and IES_i are values for IES. For example, by applying data at a latency point of 110 ms (peak latency) after TS for the IES + TS –40 ms condition in Figure 7, we obtained the following formula and calculated a and b to minimize its number:

$$1295212a^2 + 1080948b^2 - 2249122a - 1779640b + 2045030ab + 1060634$$

By solving this problem, we get $a = 0.86$ and $b = 0.007$, which indicate that the IES-evoked response does not contribute to the waveform of the IES + TS –40 ms condition at this latency point. By using this method, we could assess whether and how the control IES-evoked responses were changed in IES + TS conditions without being affected by changes of the conditioning stimulus-evoked response.

Data were expressed as the mean ± standard deviation. Differences of values among conditions were assessed with a one-way analysis of variance (ANOVA). P values of < 0.05 were considered significant.

Results

Pain rating

The mean pain rating for the control condition (IES alone) was 44.3 ± 9.3. The respective values for 11 paired stimuli conditions (IES + TS) with CTIs of –500, –300, –100, –60, –40, –20, 0, 50, 100, 300 and 500 ms were 43.1 ± 7.7, 42.5 ± 8.2, 39.7 ± 8.5, 37.4 ± 9.5, 12.7 ± 7.2, 11.1 ± 6.3, 13.7 ± 6.8, 16.8 ± 7.9, 23.6 ± 9.0, 29.1 ± 11.3 and 33.4 ± 13.9. Therefore, the pain rating was highest for the control condition and lowest for the IES + TS –20 ms condition. The difference among the twelve conditions was significant [$F(1,11) = 18.3$, $P < 0.0001$].

MEG Experiment

The mean onset latency of TS-induced magnetic fields (control TS) was 51.4 ± 7.2 ms for the first session and 49.2 ± 6.2 ms for the second session. The mean onset latency of IES-induced magnetic fields was 89.5 ± 15.4 ms for the first session and 87.5 ± 10.6 ms for the second session. The mean difference in onset latency between TS and IES was 38.1 ms (ranging from 16.2 to 59.5 ms) for the first session and 38.3 ms (from 18.2 to 54.8) in the second session. In all subjects, the field distribution of the waveform recorded from the left hemisphere (contralateral to the stimulus) following IES at the peak latency showed a single dipole pattern originating from the upper bank or bottom of the sylvian fissure corresponding to the secondary somatosensory cortex (SII)/insula region, or a two-dipole pattern originating from SII/insula and the primary somatosensory cortex (SI), similar to the results in our previous study following stimulation of the hand (Inui *et al.*, 2002b). In the right hemisphere (ipsilateral to the stimulus), clear magnetic fields were recorded in six subjects and the field distribution showed a single dipole pattern generated by activity from the SII/insula region. Figure 1 shows representative results in the first session. The nine traces in Figure 1*A* show recorded waveforms in each condition, and the seven traces in Figure 1*B* show the waveforms obtained by a subtraction of the control TS waveform from the waveform for each of the seven IES + TS conditions. The result of the subtraction clearly showed that cortical responses to IES were markedly attenuated when TS was applied at CTIs of –40, –20, 0 and 50 ms, moderately attenuated at 100 ms and slightly attenuated at 300 and 500 ms. Figures 2 and 3 show the mean time course of the amplitude of the recorded and subtracted waveforms represented as the root mean square (RMS) of all subjects. The mean peak amplitudes of the subtracted waveform of the IES + TS –500, –300, –100, –60, –40, –20, 0, 50, 100, 300 and 500 ms conditions were 100.3 ± 7.1, 100.0 ± 12.2, 99.9 ± 12.8, 76.8 ± 21.4, 34.5 ± 19.6, 20.2 ± 12.7, 23.4 ± 11.3, 35.9 ± 16.5, 45.0 ± 27.2, 68.6 ± 27.0 and 71.0 ± 26.5% of the control response, respectively. The difference among the 11 conditions was significant [$F(1,11) = 27.4$, $P < 0.0001$]. There was a significant linear correlation between the peak amplitude and pain rating (Fig. 4, $r = 0.76$, $P < 0.0001$).

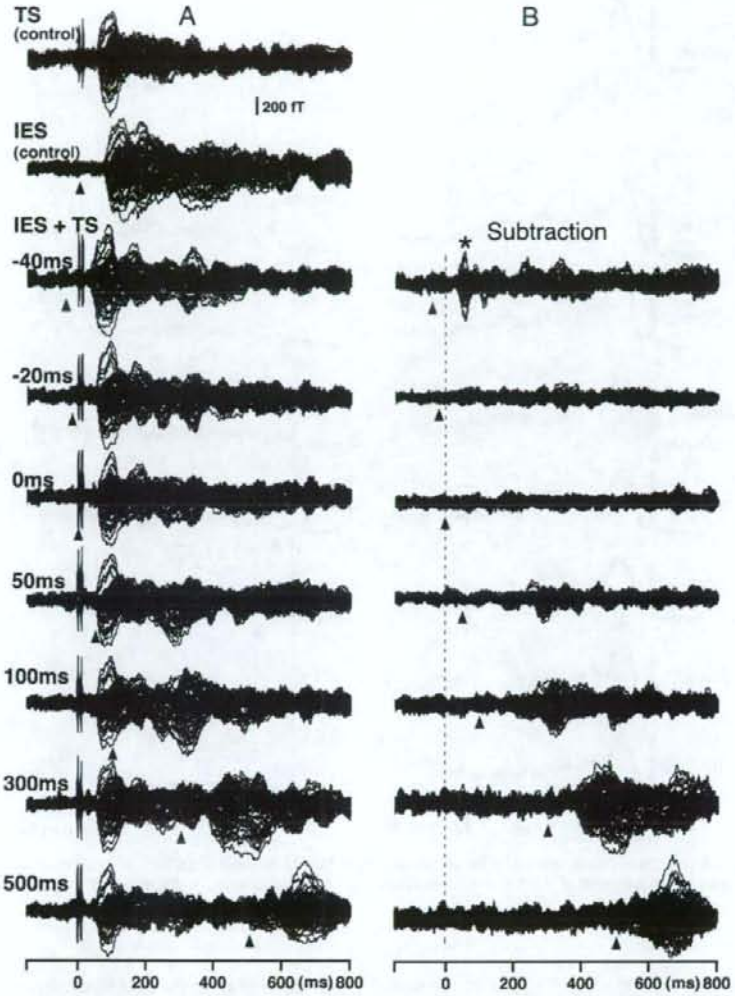

Figure 1. Effects of innocuous somatosensory stimulation on magnetic fields evoked by noxious simulation. (*A*) Recorded magnetic fields evoked by innocuous stimulation alone (control TS), noxious stimulation alone (control IES) and paired innocuous and noxious stimulations (IES + TS) applied to the back at various CTIs in a single subject (subject 1). Traces are superimposed waveforms recorded from 74 channels. (*B*) Waveforms obtained by subtraction of the control TS-evoked response from the recorded waveforms in each condition. Filled triangles indicate timing of IES. A sharp component in the subtracted waveform shown by an asterisk indicates that the IES-evoked response occurs earlier than the TS-evoked response in this condition.

Since signals evoked by TS reach the spinal cord ~5 ms earlier than signals evoked by IES due to a difference of peripheral conduction velocity between A-beta and A-delta fibers (see Materials and Methods), signals evoked by IES reach the spinal cord earlier than those due to TS in the IES + TS conditions with negative CTIs >–20 ms. Therefore, data for these IES + TS conditions are important to establishing the level in the central nervous system at which this inhibition occurs. As Figures 1 and 2 show, cortical responses to IES were almost abolished in the IES + TS –20 ms condition, indicating that the inhibition in this condition occurred at a level higher than the spinal cord. In the IES + TS –40 and –60 ms conditions in Figures 1–3, there was a sharp component around 100 ms after IES shown by an asterisk in the subtracted waveform, which indicated that the IES-induced cortical responses occurred earlier than the TS-induced responses in these conditions, and in addition, large parts of the later IES-evoked responses were almost abolished. Figure 5 shows the difference of waveform in the IES + TS –40 ms condition in detail. The waveform for the IES + TS –40 ms condition was very similar to that of the control TS, suggesting that the cortical response to TS changed little even when signals due to IES reached the cortex slightly early, and that on the other hand, IES-evoked responses were remarkably attenuated by later arriving TS-evoked signals. In Figure 6, waveforms in the IES + TS –40 ms condition of all subjects are shown.

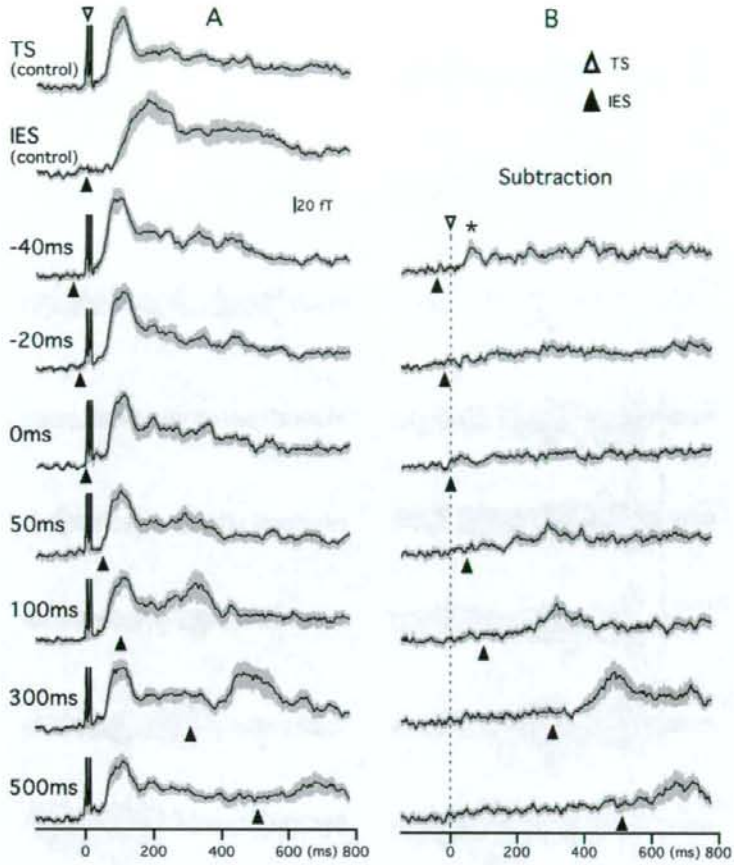

Figure 2. Group-averaged waveforms of the root mean square in the first session with seven IES + TS conditions at a CTI of −40 to 500 ms. Traces are the group-averaged time course of the amplitude of recorded (*A*) and subtracted (*B*) waveforms represented as the root mean square across 74 channels. In this and the next figure, shaded areas indicate ±1 SE width.

Next, we calculated how the control TS- and IES-evoked responses explained the waveforms of the IES + TS conditions using a least squares fit. Results from a single subject in Figure 7 showed that the waveform for the IES + TS −40 ms condition was well explained by the TS-evoked response alone except at a latency period ~50 ms after TS (90 ms after IES) where the IES-evoked response was dominant as shown by an asterisk. The time course of the coefficient *b* for the IES-evoked response was very similar to that of the subtracted waveform at a latency of 40–300 ms, which indicated the reliability of the subtraction method in this condition. Figure 8 depicts group-averaged values of coefficients *a* and *b* as functions of time among all subjects. Among the 11 IES + TS conditions, signals due to IES reach the cortex earlier than those due to TS in the −500 to −40 ms conditions, while signals due to TS reach the cortex earlier in the −20 to 500 ms conditions. Therefore, Figure 8*A*,*B* compares the effects of later arriving TS signals on the IES-evoked response and effects of later arriving IES signals on the TS-evoked response. On the other hand, Figure 8*C*,*D* compares the effects of preceding TS signals on the IES-evoked response and effects of preceding IES signals on the TS-evoked response. It is obvious from Figure 8*B* that later arriving IES signals had almost no effect on the TS-evoked response, while in marked contrast, the IES-evoked responses were strongly inhibited by later arriving TS signals (Fig. 8*A*). In Figure 8*A*, waveforms of coefficient *b* for IES in the −40, −60 and −100 ms conditions started to deviate from that of the −300 or −500 ms condition, which could be considered as a control, at ~110, 130 and 170 ms after the stimulus, indicating clearly that the IES-evoked responses in these conditions were actively inhibited by later arriving TS signals with a similar timing. In each of the three conditions, the onset latency of the inhibition corresponded approximately to the onset latency of the TS-evoked response plus 20 ms. For example, in the −60 ms condition, the onset latency of the TS-evoked cortical response was expected to be at 110 ms after IES, which was shorter by 20 ms than the latency at which the inhibition started in this condition (130 ms). When the strength of the actual IES-evoked response in each condition was expressed as the area under the curve (AUC, coefficient *b* × ms) during 50–300 ms, the AUCs for the −300,

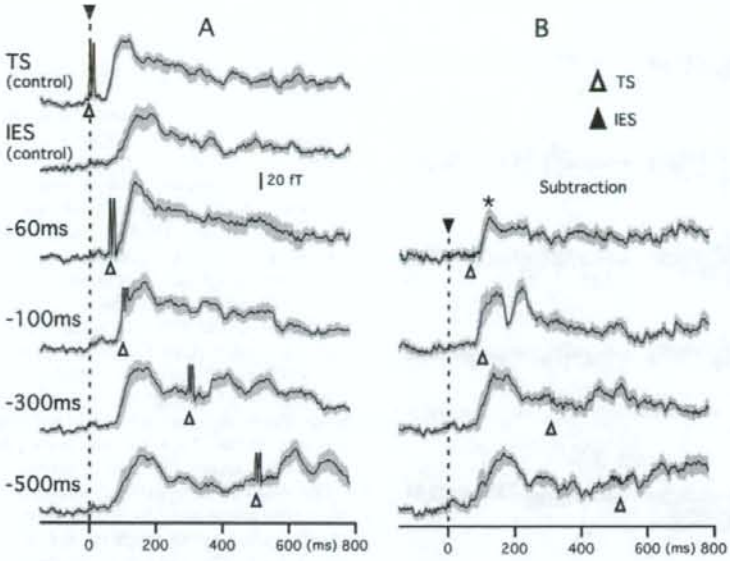

Figure 3. Group-averaged waveforms of the root mean square in the second session with four IES + TS conditions at a CTI of −500 to −60 ms.

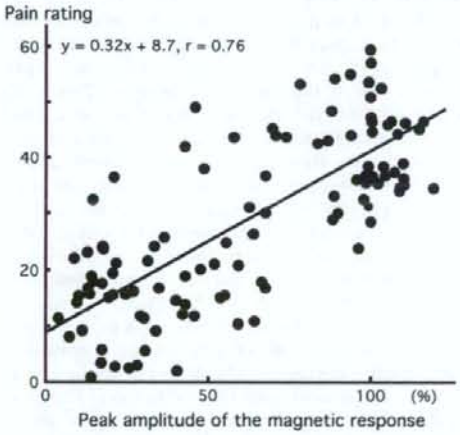

Figure 4. Correlation between the pain rating and peak amplitude of IES-induced cortical response. Data of all stimulus conditions for all subjects are plotted. Amplitudes of magnetic response are represented as a percentage of the control (IES) response. A regression line is indicated.

−100, −60 and −40 ms conditions were 103.9, 78.1, 46.5 and 22.2% of that in the −500 ms condition, respectively (Fig. 9). In the −500 ms condition, the IES-evoked response during 50–300 ms was not affected by TS at all, and therefore could be considered as a control. The AUCs for the TS-evoked response in the −20, 0, 50, 100 and 300 ms condition were 99.0, 97.4, 94.1, 103.0 and 93.1% of that in the 500 ms condition (control).

Figure 8*C,D* shows that preceding TS signals as well as preceding IES signals inhibited the IES- and TS-evoked responses, respectively. The AUCs for the IES-evoked response in the −20, 0, 50, 100, 300 and 500 ms conditions were 18.3, 15.4, 17.2, 31.6, 40.0 and 30.7% of the control value (−500ms), suggesting that the inhibition continued up to the CTI 500 ms condition. The AUCs for the TS-evoked response in the −500, −300, −100, −60 and −40 ms conditions were 57.5, 69.0, 57.8, 78.2 and 99.1% of the control value. Therefore, the inhibition of the TS-evoked response was not present when the IES- and TS-evoked signals reached the cortex simultaneously (−40 ms condition), appeared when the IES-evoked signals reached the cortex 20 ms earlier than the TS-evoked signals (−60 ms condition) and was strongest when the IES-evoked signals reached the cortex earlier than those due to TS by 60 ms (−100 ms condition). When the degree of the inhibition in these conditions was compared between the TS- and IES-evoked responses, it was significantly stronger for the TS-induced inhibition of the IES-evoked response than the IES-induced inhibition of the TS-evoked response (*t*-test, $P < 0.0001$). Like the peak amplitude in the RMS analysis, there was a linear correlation between the pain rating and AUC for IES-evoekd responses ($P < 0.0001$, $r = 0.63$). Figure 9 shows the percentage AUC relative to the control for the TS- and IES-evoked response in all conditions.

Discussion

This is the first report to show tactile-induced pain inhibition at the cortical level. A previous paper from our laboratory (Kakigi and Watanabe, 1996) examined effects of tactile stimuli applied to the fingers on vertex potentials evoked by laser beams applied to the dorsum of the same hand. No effects were found when a stroke by a soft wad of tissue paper was used as a tactile stimulus, while laser-evoked potentials were significantly inhibited when continuous vibrotactile stimuli (500 Hz) was used. The results suggest that the timing of the conditioning stimulus is important to its inhibitory effects on pain-evoked brain responses as the present study showed.

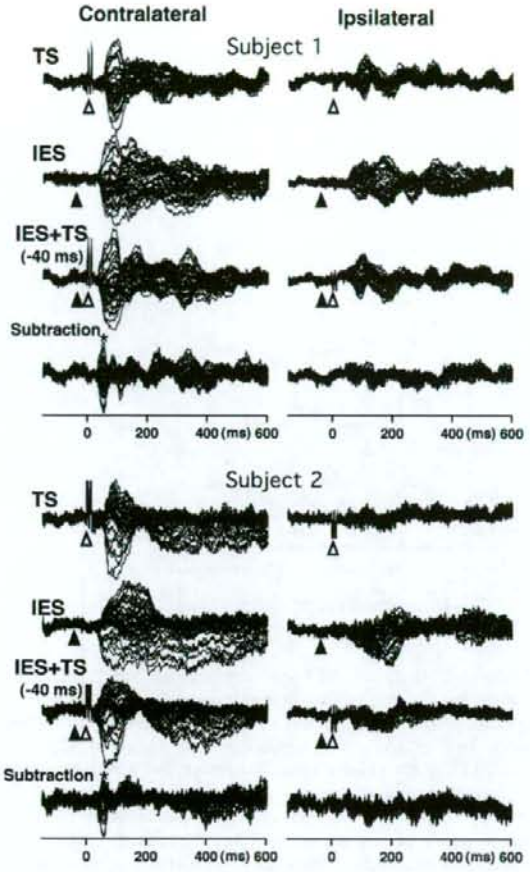

Figure 5. Inhibition of the IES-evoked response by TS delivered 40 ms later than IES. Waveforms recorded by two probes (contralateral and ipsilateral hemispheres) are separately shown in this figure. Open and filled triangles indicate timing of TS and IES, respectively. Note that waveforms recorded from both hemispheres are very similar between the TS and IES + TS conditions in both subjects except that waveforms in the IES + TS condition have activity due to IES at the very beginning of the evoked component as shown by an asterisk.

It is probable that the failure to find an inhibitory effect of a stroke of the fingers on laser-evoked potentials was due to the non-time-locked conditioning stimuli. An important technical issue of the present study was the use of an intra-epidermal electrical stimulation (IES) method that could selectively activate A-delta fibers with constant activation timing in each trial, and therefore enabled us to study interactions between two different modalities with precise timing. In previous studies, we confirmed that signals evoked by IES are conveyed through peripheral A-delta fibers at a conduction velocity of ~15 m/s (Inui *et al.*, 2002a,b). In this study, the latency difference of evoked cortical activity between TS and IES was ~38 ms, which was almost consistent with the estimated latency difference based on the reported conduction velocities of peripheral A-beta and A-delta signals in the human spinal cord. The sharp pricking sensations without any tactile sensations evoked by IES also support that IES activates A-delta fibers selectively. Furthermore, the present result itself showed that IES selectively stimulates A-delta fibers. If IES activates A-beta and A-delta fibers simultaneously (i.e. CTI = 0 ms), the responses evoked should be similar in latency to those evoked by TS.

As possible mechanisms underlying pain relief by vibrotactile stimulations, those operating at the periphery (Campbell and Taub, 1973), dorsal horn of the spinal cord (Melzack and Wall, 1965) and other regions of the central nervous system (Melzack, 1971) have been postulated. In the major hypothetical mechanisms at the spinal level, it has been suggested that a 'gate control' mechanism exists in the dorsal horn of the spinal cord, where signals through large diameter fibers are said to inhibit the central transmission of signals through small diameter fibers (Melzack and Wall, 1965). In the present study, noxious stimuli-induced cortical responses were equally inhibited by simultaneous (CTI 0 ms) and delayed (CTI –40 and –20 ms) innocuous stimulations, excluding the possibility of peripheral mechanisms. The findings of a substantial inhibition of the IES-induced response in the IES + TS conditions with a negative CTI of > –20 ms suggest that the inhibition occurs without any contribution at the spinal level, including descending inhibitory actions on spinal neurons, at least in these conditions because signals evoked by IES reach the spinal cord earlier than those evoked by TS. The findings in the IES + TS –100 to –40 ms conditions indicate that the inhibition occurs at the cortical level. Although our results could not clarify the extent to which the spinal mechanisms contributed to the inhibition in the IES + TS 0 to 500 ms conditions, the powerful inhibition in the IES + TS –40 ms and IES + TS –20 ms conditions and the low pain rating for the IES + TS –20 ms condition imply that any inhibitory action at the spinal cord is weak. This notion is consistent with the fact that, in general, repetitive and high intensity stimulations of a peripheral nerve, which activate both A-beta and A-delta fibers, are required to suppress noxious stimuli-evoked responses in the dorsal horn neurons in animal studies (Cervero *et al.*, 1976; Chung *et al.*, 1984; Lee *et al.*, 1985). Whitehorn and Burgess (1973) showed that primary afferent terminals of a particular sensory fiber type are depolarized by activity arising in fibers of the same type. Similar findings were reported by Brown and Hayden (1972). Therefore, inhibition of the nociceptive neurons in the dorsal horn by repetitive stimulation of a peripheral nerve at noxious intensities or by applying intense mechanical stimuli to the skin seems to be largely due to presynaptic inhibition by A-delta or C fiber inputs rather than A-beta fibers. The notion that nociceptive neurons in the dorsal horn cannot be easily suppressed by signals from low-threshold mechanoreceptors is supported by the findings of Manfredi (1970) and Pomeranz (1973), who examined post-synaptic activity of the dorsal horn neurons in the lateral tract in cats and found no inhibitory effects of A-beta fiber inputs. The fact that stimulation of C-fibers generates a primary afferent depolarization but not a primary afferent hyperpolarization in the spinal cord (Zimmermann, 1968) also does not support the gate control theory.

Since the main component of the evoked magnetic fields in the present study originated mainly from SII and SI, and since SI and SII were sequentially activated by IES in our previous study (Inui *et al.*, 2003a,b), the inhibitory action should take place in SI neurons or in both SI and SII neurons. Several lines of evidence show that SI nociceptive neurons play a role in the discriminative aspect of pain (Kenshalo and Willis, 1991;

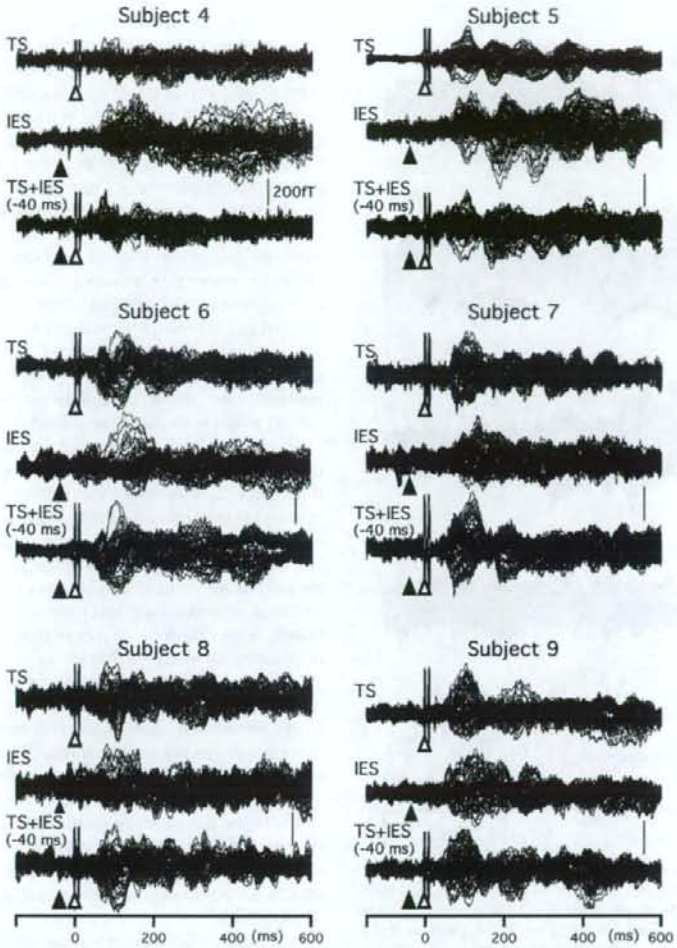

Figure 6. Waveforms in the IES + TS −40 ms condition of six subjects. Note that the waveform in the IES + TS condition is similar to the waveform in the control TS condition. Waveforms of three other subjects in this condition are shown in Figures 1, 5 and 7.

Bushnell *et al.*, 1999). Since the IES-evoked later components, which originated from the insular cortex, medial temporal area around the amygdala or hippocampus and cingulate cortex (Inui *et al.*, 2003a), were attenuated as well as the main early component in this study, there might be direct inhibitory actions on these areas independent of those on SI and SII. The origin of the inhibitory action is unclear from the present results, but TS-driven thalamic and cortical activities are candidates. The present study suggests that activation of the tactile pathway at a certain level higher than that in the spinal cord can inhibit cortical responses to noxious stimuli. In the major tactile pathway, the dorsal column is known to alleviate chronic pain when electrically stimulated (Shealy *et al.*, 1970). In addition, behavioral responses to noxious stimuli in rats (Saadé *et al.*, 1986) as well as experimentally evoked pain in humans (Marchand *et al.*, 1991) are reduced by stimulation of the dorsal column. Although the mechanisms responsible for pain inhibition on stimulation of the dorsal column are still unclear, the nociceptive thalamus–SI pathway might be modulated. Larson *et al.* (1974) showed that evoked potentials recorded in human somatosensory cortex, and those recorded in monkey ventroposterior lateral nucleus (VPL) of the thalamus and sensorimotor cortex are attenuated by stimulation of the dorsal column. Bantli *et al.* (1975) examined the effects stimulating the dorsal column on the cortical responses to stimulation of the ventral quadrant of the spinal cord in monkeys and found that evoked activities in both SI and SII were inhibited, similar to the present results.

In the main tactile pathway, the VPL and the ventroposterior medial nucleus (VPM) of the thalamus are shown to reduce experimentally induced pain in humans when electrically stimulated (Marchand *et al.*, 2003). In addition, electrical stimulation of VPL/VPM is effective in relieving chronic pain (Hosobuchi *et al.*, 1973; Mazars *et al.*, 1973) and allodynia

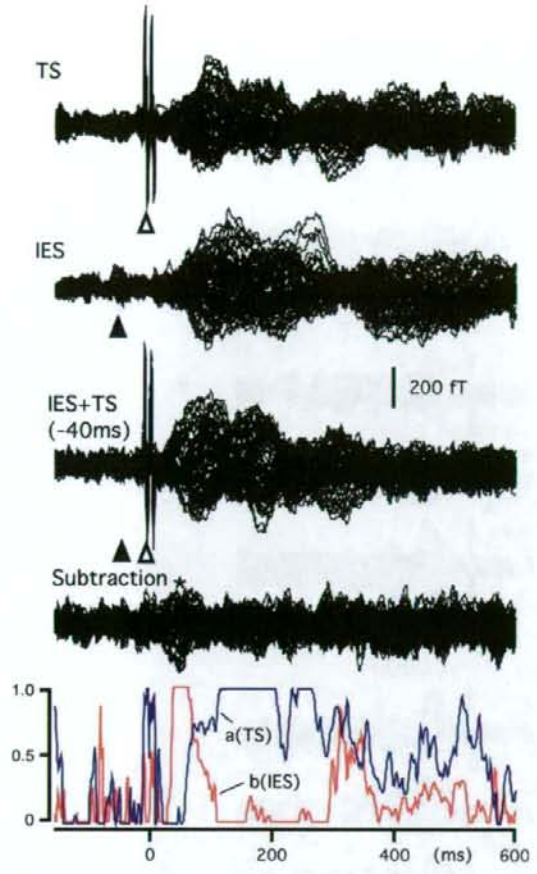

Figure 7. Contribution of the control TS- and IES-evoked responses to the responses evoked by paired stimuli. By use of a least squares fit, we calculated how the control TS and IES waveforms explained the waveforms in IES + TS conditions. The bottom traces show the time course of coefficients for TS (*a*) and IES (*b*). The result of this case (subject 3) shows that magnetic fields evoked by paired stimuli can be explained by only the control TS-evoked response except at a latency period of ~30–60 ms after TS, where the control IES-evoked response alone can explain the response shown by an asterisk.

in rats (Kupers and Gybels, 1993). Like stimulation of the peripheral nerve and dorsal column, the stimulation of VPL/VPM usually elicits paresthetic sensations without sensations of pain. In addition, the electrode must be placed in the somatotopic part of the VPL/VPM nuclei that represents the painful site to obtain pain relief (Gybels, 2001), which mimics rubbing a bruised area to reduce pain. These thalamic nuclei send dense projections to SI. Therefore, this thalamo-cortical pathway may mediate analgesia produced by thalamic stimulation. The fact that successful stimulation in patients with chronic pain produces localized paresthetic sensations in the painful area and increases cerebral blood flow in SI and the thalamic region stimulated (Katayama *et al.*, 1986; Duncan *et al.*, 1998) appears to support the involvement of the VPL/VPM-SI pathway in pain relief by thalamic stimulation. The inhibition of nociceptive SI neurons by sensory thalamus stimulation may explain why electrical stimulation of this area rarely produces painful sensations though VPL/VPM contains considerable numbers of nociceptive neurons (Kenshalo *et al.*, 1980; Chung *et al.*, 1986; Bushnell *et al.*, 1993; Apkarian and Shi, 1994). Davis *et al.* (1996) examined effects of microstimulation in the ventrocaudal nucleus of the thalamus of patients with chronic pain and found that the stimulation frequently evoked sensations of pain in patients with post-stroke pain but only paresthetic sensations in non-stroke patients. The increased incidence of thalamic-evoked pain in such patients may be due to the relative dominance of the nociceptive thalamus-SI pathway following loss of low-threshold mechanoreceptor thalamic neurons or reduced tonic inhibition of thalamic or cortical nociceptive neurons. This notion is similar to Mazars's original hypothesis of pain relief by thalamic stimulation that when pain is due to a lack of proprioceptive information reaching the thalamus from the damaged region, it might be controlled by thalamic stimulation in place of physiological stimuli running through the dorsal column.

Another possible explanation of tactile-induced pain inhibition is that tactile inputs inhibit nociceptive brain areas other than the VPL–SI pathway via thalamo-thalamic, thalmo-cortical or cortico-cortical inhibitory projections. For example, Craig *et al.* (1994) demonstrated a very high concentration of pain- and thermo-specific neurons in the posterior part of the ventral medial thalamic nucleus (VMpo) in monkeys, which has dense lamina I spinothalamic tract terminations. In lamina I of the dorsal horn, there is a population of neurons specifically responding to noxious stimuli in cats (Christensen and Perl, 1970) and monkeys (Kumazawa *et al.*, 1975) similar to VMpo neurons. In addition, stimulation around VMpo elicits localized sharp painful sensations and nociceptive-specific neurons are recorded in this region in humans (Craig, 2003). VMpo projects to the dorsal part of the insula and other cortical areas such as area 3a of SI (Craig, 2003). Therefore, VMpo and its projection sites may be the target in tactile-induced inhibition of pain. We considered that a thalamo-cortical pathway via VMpo is one candidate for sites receiving inhibitory effects, although some recent studies questioned the existence of this nucleus (Willis *et al.*, 2002).

Previous studies suggested one primary site of pain processing in the dorsal posterior insula (Craig, 2003; Vogel *et al.*, 2003) where VMpo projects. In fact, activity from the dorsal part of the insula contributes to creating the major magnetic component evoked by IES (Inui *et al.*, 2003a), which was almost completely suppressed by TS in the present study. As for activity in area 3a, Tommerdahl *et al.* (1996) demonstrated clusters of nociceptive neurons that show an augmenting response to repeated brief heat stimuli in monkeys. In addition, they showed that activation in area 3a by noxious heat stimuli was accompanied by a reduction of activity in areas 3b and 1 produced by innocuous mechanical simulation, which was likely mediated by long-distance horizontal connections that link area 3a and areas 3b/1. Given the inhibitory cortico-cortical projections from area 3a to areas 3b/1 in the pain-touch interaction, it seems possible that IES-evoked area 3a activity was inhibited by similar cortico-cortical projections from areas 3b/1 in the present study. Our data that the onset latency of the inhibition of the IES-evoked response by TS was ~20 ms later than the arrival of TS signals to the cortex (IES +TS conditions from −100 to −40 ms) are consistent with such a cortico-cortical inhibition. However, activation of neurons in the bottom of the sulcus creates

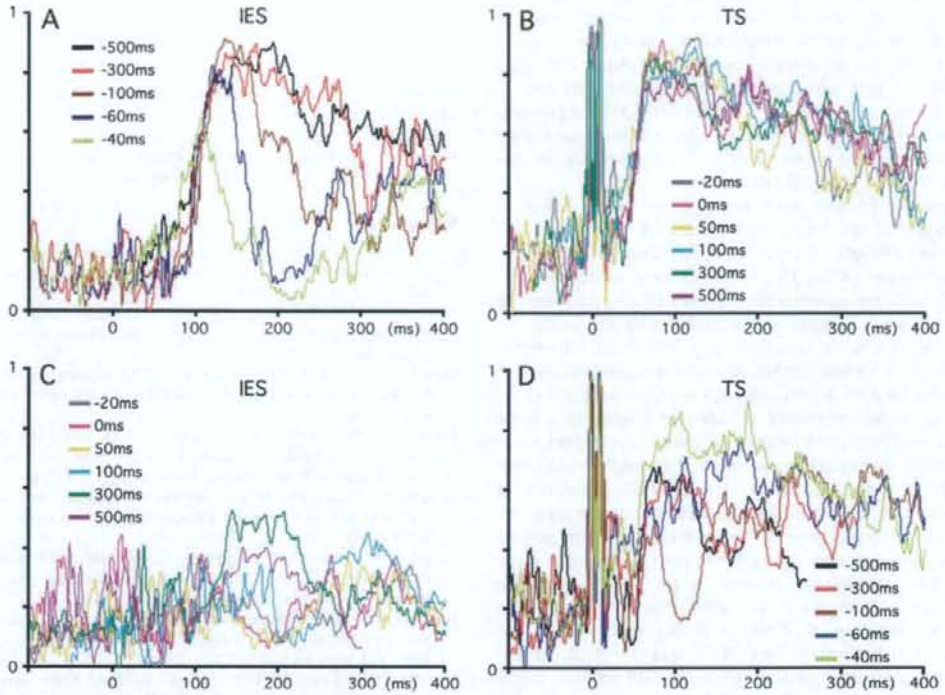

Figure 8. Group-averaged time course of the coefficients for TS and IES. (*A*) Effects of later arriving TS signals on the IES-evoked response. (*B*) Effects of later arriving IES signals on the TS-evoked response. (*C*) Effects of preceding TS signals on the IES-evoked response. (*D*) Effects of preceding IES signals on the TS-evoked response.

a dipole with a radial orientation that is difficult detect by MEG, therefore our recorded magnetic fields might not reflect activity from area 3a.

The role of SII in pain perception is unclear, largely due to the lack of unit study findings on nociceptive neurons in this area. In marked contrast with human neuroimaging studies in which activations in SII are constantly found after noxious stimulation, nociceptive neurons are rarely encountered in SII in animal studies (for review, see Schnitzler and Ploner, 2000). For example, the proportion of nociceptive neurons was 4% (5 of 123 neurons) in a study by Dong *et al.* (1989). The present finding of powerful inhibition by tactile inputs of responses to noxious stimuli in SII suggests that the paucity of nociceptive neurons in SII in animal studies might be a result of the use of a non-selective intense mechanical stimulation that activates low-threshold mechanoreceptors as well as nociceptors, since the present results showed that noxious stimuli-evoked SII activity was markedly inhibited when an innocuous stimulus was applied simultaneously (CTI 0 ms). If a selective noxious stimulation is used as a searching stimulus, a larger number of nociceptive neurons might be found in SII.

Although the pain rating was correlated with both the peak amplitude of the IES-evoked response (subtracted) and the integral strength of the coefficient for the IES-evoked response during the 50–300 ms latency, data in some conditions did not show a simple linear correlation between them. The rating for the IES + TS −40 ms condition (12.7) was not so different from that for the −20 ms (11.1) and 0 ms (13.7) conditions, while

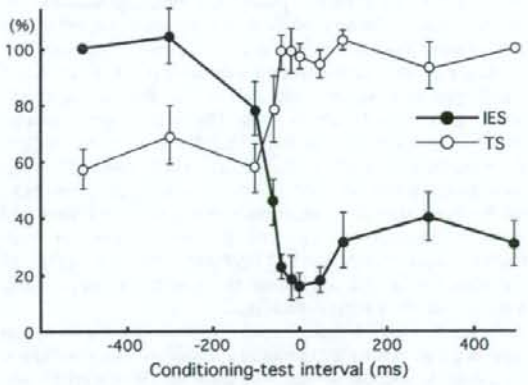

Figure 9. Amplitudes of the IES- and TS-evoked response represented as an integral of the respective coefficient value. Each value is the percentage of the area under the curve (AUC) during a latency period of 50–300 ms relative to that in the control condition (500 ms condition for TS and −500 ms condition for IES). Vertical bars indicate ±1 SE.

the peak amplitude of the −40 ms condition (34.5% of the control) was apparently greater than that of the −20 ms (20.2%) and 0 ms (23.4%) conditions, due to the presence of an early sharp component that escaped the inhibition in the −40 ms condition. This result implies that the early sharp component in the −40 ms condition did not help to produce painful sensations.